Revised, August 2001

Dynamics in fine particle magnets

J. van Lierop[1] and D.H. Ryan

Physics Department and Centre for the Physics of Materials,

McGill University, 3600 University Street, Montreal, Quebec H3A 2T8, Canada.

(February 6, 2002)

Abstract

Several magnetic fine particle systems have been studied with selective excitation double Mössbauer (SEDM) spectroscopy. Static disorder, collective excitations and superparamagnetic spin flips are all detected and their contributions quantified. Zero-field muon spin relaxation spectroscopy has been used to confirm these observations in one sample. A theoretical description of SEDM spectra in static and dynamic disordered magnetic systems is presented.

PACS numbers: 75.50.Tt, 76.60.Es, 76.80.+y, 76.75+i

I. INTRODUCTION

The moment of a single domain particle is blocked with the magnetization fixed along the particle easy axis at low temperatures. With rising temperature, collective excitations [2] develop (oscillations of the magnetization vector around the easy axis) followed by superparamagnetic 180° moment flips about the easy axis. The temperature where the transition between collective excitation and superparamagnetism occurs is the blocking temperature, T_B, of a single domain particle.

Any real fine particle system is inevitably composed of a collection of different sized single domain particles. All particle moments are blocked at the lowest temperatures, however, with increasing temperature, the moments of the smaller particles will begin to experience collective excitations. Additionally, with a further rise in temperature, the smaller particle moments will become superparamagnetic, moments of intermediate sized particles will undergo collective excitations, and the moments in the largest particles will remain blocked. The balance of particle moment behavior shifts towards superparamagnetism with increasing temperature until the moments of all particles undergo spin flips. This wide variety of magnetic behavior is further complicated by inter-particle interactions [3] arising from the difficulty in controlling particle dispersal. Usually of a dipolar nature, inter-particle interactions will affect the energy necessary for moment flips (the effective anisotropy energy), and change the temperature at which a particle becomes superparamagnetic. A final complication derives from the chemical or grinding procedures used to prepare most fine particle systems. These lead to the introduction of varying degrees of static disorder which can further affect T_B, anisotropy energy, and also build in a static disorder contribution that can mimic the dynamic disorder that arises from collective moment fluctuations.

The principal difficulty in measuring the above magnetic properties in fine particle systems resides in the different sensitives of experimental techniques, which are generally a function of the measuring time of the experimental probe. For example, magnetization measurements are dominated by the response of the larger, slower particle moments, while the majority of the signal in ac susceptibility (χ_{ac}) comes from particle moments that are close to their blocking temperature. Transmission Mössbauer spectroscopy is one of the more useful techniques for probing the magnetic behavior in fine particle systems [3], however, quantitative comparison with other techniques has only recently become possible with the development of a model that properly describes the complete range of magnetic behavior in the spectra of fine particle systems [4,5]. Since the ability to separate the static and dynamic magnetic signals in a fine particle system is the chief concern, another useful experimental technique is zero-field muon spin relaxation (ZF-μSR) spectroscopy. The muon is a sensitive local magnetic probe. ZF-μSR provides a Kubo-Toyabe type lineshape in the early time channels from static magnetic behavior [6], and an exponential decay in later time channels from spin dynamics. The frequency range covered by ZF-μSR is broader than that of Mössbauer spectroscopy, but the two techniques have substantial overlap and provide complementary information so that results obtained using μSR can be compared directly with those from Mössbauer effect experiments.

Ideally, one needs an experimental probe that is both sensitive to the full range of magnetic behavior exhibited by a fine particle system, and also provides distinct signatures for static and dynamic magnetic properties that are independent of particle size distributions. Fortunately, the modified Mössbauer technique of selective excitation double Mössbauer (SEDM) spectroscopy meets the requirements for studying magnetic fine particle systems [7–9]. Additionally, when superparamagnetic moment reversals are observed in SEDM spectra, a *model independent* measure of the flip rate is provided.

In contrast to a conventional transmission Mössbauer experiment where the γ-ray absorption from a sample is measured as the γ energy is swept across a range of values, during a SEDM experiment the sample is pumped at a fixed, single energy, and the re-emitted radiation is analyzed. Our recent innovations to the SEDM technique (e.g. a three order of magnitude improvement in effective counting times, and a spectrometer that can run continuously without periodic energy calibrations [8,9]), have removed it from its standing as a fringe spectroscopic technique, and allowed us to apply it to problems of current interest [7,8]. The static magnetic field present at the ^{57}Fe nucleus in a magnetically ordered material induces hyperfine splittings in the $I_g = \frac{1}{2}$ ground state and the $I_e = \frac{3}{2}$ excited state, and selection rules ($\Delta m_I = 0, \pm 1$) mean that only six of the eight possible transitions are allowed. These hyperfine splittings result in the six-line spectrum that is observed in transmission Mössbauer spectra, where each line corresponds to an energy transition of the magnetic hyperfine field. As pumping a specific energy transition in a magnetic sample is fundamental to SEDM, the sample must show distinct hyperfine splittings (i.e. a multi-line spectrum). By pumping a specific energy transition, SEDM essentially breaks the left-right symmetry of a transmission Mössbauer spectrum, so that the time-dependent moment behavior that is masked by this left-right symmetry can be exposed. For example, the selection rules allow only a single transition from the $m_e = -\frac{3}{2}$ state, so in a material with a unique static magnetic field, e.g. α-Fe, the radiation re-emitted when the excited nucleus decays to the ground state is at the same energy as the pump energy. A single, sharp line is observed in the SEDM spectrum for this case. However, if (for example) there is a 180° moment flip during the lifetime of the excited nucleus, the field will reverse, the projection of I_e onto that field will change sign, and the populated state becomes $m_e = +\frac{3}{2}$. Two lines are observed in the SEDM spectrum for this case, one at the pump energy, and an other at the energy that is opposite to the pump energy [8]. The relative intensity of the two lines is a direct, model independent, measure of the flip rate.

We have examined two ferrofluids with median particle diameters of 4.5 nm and 6.0 nm using SEDM spectroscopy, and compared the observed magnetic behavior with results from our conventional transmission Mössbauer spectroscopy and χ_{ac} study of the ferrofluids [5], and a ZF-μSR study of a polysaccharide iron complex [10]. Static moments, collective magnetic excitations, and superparamagnetic spin flips have each provided distinct spectral features. SEDM measurements of T_B and spin flip relaxation rates are in agreement with those determined from transmission Mössbauer results.

II. EXPERIMENTAL METHODS

SEDM spectroscopy uses two Mössbauer resonant scattering events to measure the differential cross-section of resonant nuclei in the sample. The first resonant event pumps a selected nuclear transition in the hyperfine nuclear structure and populates a specific excited state. The second resonant event occurs during the de-excitation of the nucleus back to the ground state.

The SEDM apparatus requires two Doppler modulators, shown schematically in Fig. 1. One is used to drive the single line, 1 GBq ^{57}Co**Rh** Mössbauer source at a constant velocity (CVD), populating the desired nuclear sublevel in the sample. The other velocity transducer runs in constant acceleration (CAD) mode and carries a single-line resonant conversion electron detector (CED) used to energy-analyze the scattered radiation from the sample. A complete description of our SEDM apparatus and its operation can be found in Ref. [9].

Since magnetic fine particle systems exhibit a rich variety of magnetic phenomena, it is necessary to establish the individual signatures of static magnetic fields, static magnetic disorder, and dynamic disorder before attempting to describe the temperature dependent magnetic behavior of single domain particles. The effects of a unique magnetic environment are most easily studied using α-Fe, a material with a bcc lattice where Mössbauer nuclei are exposed to a single, 33 T hyperfine field. Selection rules allow only a single transition from the $m_e = -\frac{3}{2}$ state, so in α-Fe with a unique static magnetic field, the radiation re-emitted when the excited nucleus decays to the ground state is at the same energy as the pump energy. A single, sharp line is observed in the SEDM spectrum, as shown in the top panel of Fig. 2. This instrument-limited linewidth is set by the properties of the nuclear transition, with a small contribution from instrumental effects. The line position in the SEDM spectrum is in perfect agreement with the position of line #1 in the α-Fe transmission spectrum.

A sample of a-$Fe_{80}B_{20}$ was used as an example of static disorder. The SEDM spectrum obtained while driving line #1 (middle panel in Fig. 2) again shows a single line centered on the energy set by the constant velocity drive and in perfect agreement with the position of line #1 in the transmission spectrum of the same sample [7]. A single line is also required by the selection rules. Closer examination of the data reveals that the observed SEDM line is significantly broader than the instrument-limited one obtained from α-Fe. The effects of static disorder on the SEDM spectrum are thus clear: The selection rules for a static magnetic hyperfine field are followed, however there is a contribution to the apparent linewidth from the range of *static* magnetic environments present in the sample. If the effects of the hyperfine field distribution are properly included (see below), then the instrumental linewidth is recovered.

Finally, a SEDM spectrum of the 6.0 nm ferrofluid at 80 K shows the effects of time-dependent magnetism. Superparamagnetism involves a 180° moment flip during the lifetime of the excited nucleus, and the field reverses direction, with the projection of I_e onto that field changing sign, so the populated state becomes $m_e = +\frac{3}{2}$. Two lines are now observed in the SEDM spectrum (Fig. 2, bottom panel), one at the pump energy (~ -8 mm/s), and a second at the energy that is opposite to the pump energy ($\sim +8$ mm/s).

With the SEDM spectral signatures of static and dynamic disorder characterized, we have investigated the spin dynamics in two ferrofluids with average particle sizes of 4.5 nm and 6.0 nm. These commercial materials were prepared by mechanical grinding of bulk magnetite (Fe_3O_4) under oil in the presence of a surfactant [11]. $T_B = 50 \pm 5$ K for the 6.0 nm ferrofluid and $T_B = 30 \pm 5$ K for the 4.5 nm ferrofluid were determined using a multiple-level relaxation transmission Mössbauer spectroscopy formalism combined with an exact analytic expression for the relaxation time of a single domain magnetic particle [12] and a log-normal particle size distribution [5]. These T_Bs were confirmed from the frequency dependence of χ_{ac} data, assuming a 10^{-8} s measuring time for the Mössbauer measurements [5]. Energy calibration was done with a room temperature α-Fe foil. The left-most line in the spectrum was pumped as it has the largest absorption cross-section, thus maximizing the signal and reducing collection times. Sample temperatures of 20 to 200 K were obtained with a closed cycle refrigeration system. Typical counting times were 20 days.

III. LINESHAPE CALCULATIONS

Lineshape models for the different physical situations are necessary to extract quantitative information from the SEDM spectra. SEDM is essentially a modified scattering Mössbauer experiment, and the description of a scattering Mössbauer experiment is much more involved than for a transmission Mössbauer experiment. It is necessary to establish a formalism to describe the resonant scattering that occurs during a SEDM experiment where only a single transition is driven, and two resonant Mössbauer events occur during the measurement. A complete description of the SEDM process in a sample with a single, static B_{hf} [13] has been developed. This model calculates the energy distributions of scattered radiation from sample and energy analyzer, and integrates these energy distributions to describe the effects of sample and detector thicknesses (a single-line $Na_4Fe(CN)_6{\cdot}10H_2O$ absorber attached to the CAD with a standard proportional counter behind it [13,14] was used in their SEDM apparatus) and thus determines the SEDM pattern. This approach was necessary in order to include sample thickness effects. The SEDM experiments reported here were carried out on very thin metal alloys (melt spun ribbons $\sim 20\,\mu$m thick) and two ferrofluids with low iron contents [11]. No thickness effects were observed in transmission Mössbauer or SEDM spectra. A simpler description assuming Lorentzian lineshapes for the SEDM spectra of thin samples was therefore devised. However, since we performed SEDM experiments on samples with static disorder, it was necessary to extend the SEDM lineshape model to include the effects of a static distribution of hyperfine fields.

To describe a SEDM lineshape, two energies need be accounted for. One is the CVD transducer velocity that defines the energy of the populated sublevel in the sample. The other is the velocity of the CAD during its energy analysis of scattered radiation from the sample. In analyzing a SEDM experiment it is important to know the energy distribution of the source radiation, the energy distribution of the scattered radiation from the sample, and the energy resolution of the detector. These items are characterized by the linewidths of these processes.

When a material with a single, static hyperfine field is examined using SEDM, the lineshape is described by the expression:

$$
\begin{aligned}
I(E,S) &= \frac{(\Gamma_D/2)^2}{E^2-(\Gamma_D/2)^2} \\
&\times\left(\sum_{i=1}^{6}\frac{W_{i,i}(\alpha)(\Gamma/2)^2}{(E-E_i)^2+(\Gamma/2)^2}\frac{(\Gamma_b/2)^2}{(E-S)^2+(\Gamma_b/2)^2}\right. \\
&+\sum_{i=2}^{3}\frac{W_{i,i+2}(\alpha)(\Gamma/2)^2}{(E-E_{i+2}-G)^2-(\Gamma/2)^2}\frac{(\Gamma_b/2)^2}{(E-S-G)^2+(\Gamma_b/2)^2} \\
&+\left.\sum_{i=2}^{3}\frac{W_{i+2,i}(\alpha)(\Gamma/2)^2}{(E-E_{i+2}+G)^2-(\Gamma/2)^2}\frac{(\Gamma_b/2)^2}{(E-S+G)^2+(\Gamma_b/2)^2}\right)
\end{aligned}
\tag{1}
$$

where S is the CVD velocity, E the CAD velocity and E_i the energy of each spectral line (see Fig. 4). Γ_b represents the linewidth of the source, Γ the linewidth of the excited state in the sample and Γ_D is the instrumental linewidth of the CED (or more generally, the energy analyzer), and $G = E_4 - E_2 = E_5 - E_3$. $W(\alpha)$ represent the angular distribution of resonantly scattered radiation, where $\alpha = 90°$ is the scattering angle (Fig. 3). For a powder sample we have [13]

$$
\begin{aligned}
W_{1,1} &= W_{6,6} = \left(\frac{3}{8\pi}\right)^2\frac{1}{4}\left(\frac{26+2\cos^2(\alpha)}{15}\right) \\
W_{2,2} &= W_{5,5} = \left(\frac{3}{8\pi}\right)^2\frac{4}{9}\left(\frac{6+2\cos^2(\alpha)}{15}\right) \\
W_{3,3} &= W_{4,4} = \frac{1}{9}W_{1,1} \\
W_{2,4} &= W_{4,2} = W_{3,5} = W_{5,3} = \left(\frac{3}{8\pi}\right)^2\frac{1}{9}\left(\frac{14-2\cos^2(\alpha)}{15}\right)
\end{aligned}
\tag{2}
$$

which is appropriate when describing the SEDM spectra of the ferrofluids, as the moments are frozen in a random orientation in the carrier-liquid at temperatures below ~200 K (R_{25}=2, i.e. the transmission spectra line intensities follow a 3:R_{25}=2:1:1:R_{25}=2:3 ratio for lines #1 through #6). For the α-Fe foil and melt-spun ribbon samples, a bulk magnetization direction results in transmission Mössbauer spectra with a $R_{25} \neq 2$. It is not possible to calculate the W's for this more complex situation. Determining W becomes a difficult structure problem where at least three transmission Mössbauer spectra need to be collected with the incident γ-rays at different orientations with respect to sample [15]. For these experiments, the SEDM sample was always mounted with the ribbons horizontal with respect to the incident γ-rays or, for the α-Fe foil, its roll direction horizontal with respect to the incident γ-rays. Using the 3:R_{25}:1:1:R_{25}:3 ratios from transmission Mössbauer spectra fits to denote $W_{1,1}$:$W_{2,2}$:$W_{3,3}$:$W_{4,4}$:$W_{5,5}$:$W_{6,6}$ correctly described the SEDM spectra.

Examining the top panel of Fig. 2, we find that Eqn. 1 correctly predicts the SEDM lineshape for a single, static magnetic environment. With $E_1 = -5.3123$ mm/s measured from a transmission Mössbauer spectrum, and the detector linewidth independently characterized [9]. The only fitted parameters were the observed linewidth Γ_s which includes all of the instrumental resolution ($\Gamma_s = \Gamma + \Gamma_b + \Gamma_D = 0.165 \pm 0.001$ mm/s), along with the baseline and an intensity scale factor.

When describing a SEDM spectrum of a sample with static disorder, additional information is required. The distribution of hyperfine fields, $P(B_{hf})$, determined from a transmission Mössbauer spectrum allows the energy of a selected sublevel to be calculated for each hyperfine field in $P(B_{hf})$. The source linewidth, Γ_b, and pump energy determines the particular region of the hyperfine field distribution that is accessed. The final lineshape reflects a convolution of the source linewidth with $P(B_{hf})$. The continuum of B_{hf}'s in the sample is approximated by a discrete series of values and was obtained from a fit of the transmission Mössbauer spectrum. One SEDM sub-spectrum is calculated for each B_{hf}, and the final lineshape is constructed from a weighted sum of these sub-spectra. This correctly describes the SEDM spectrum of a material with static disorder. The lineshape is given by:

$$I(E,S) = \sum_{B_{hf}=0}^{B_{hf}^{max}} P(B_{hf}) \times \frac{(\Gamma_D/2)^2}{E^2 - (\Gamma_D/2)^2} \times \tag{3}$$
$$\Bigg(\sum_{i=1}^{6} \frac{W_{i,i}(\alpha)(\Gamma/2)^2}{(E-E_i)^2 + (\Gamma/2)^2} \frac{(\Gamma_b/2)^2}{(E-S)^2 + (\Gamma_b/2)^2}$$
$$+ \sum_{i=2}^{3} \frac{W_{i,i+2}(\alpha)(\Gamma/2)^2}{(E-E_{i+2}-G)^2 - (\Gamma/2)^2} \frac{(\Gamma_b/2)^2}{(E-S-G)^2 + (\Gamma_b/2)^2}$$
$$+ \sum_{i=2}^{3} \frac{W_{i+2,i}(\alpha)(\Gamma/2)^2}{(E-E_{i+2}+G)^2 - (\Gamma/2)^2} \frac{(\Gamma_b/2)^2}{(E-S+G)^2 + (\Gamma_b/2)^2} \Bigg)$$

The transmission spectrum of a-$Fe_{80}B_{20}$ exhibits the usual broadened six-line pattern of a metallic glass with a broad hyperfine field distribution, P(B_{hf}). SEDM data obtained driving line #1 (middle panel in Fig. 2) shows a single broad line which may be fitted assuming the same P(B_{hf}) determined from the transmission spectrum. Γ_b and P(B_{hf}) correctly predict the SEDM lineshapes with a fitted linewidth of $\Gamma_s = 0.165 \pm 0.002$ mm/s. This value includes all of the instrumental parameters: the CED energy resolution, and the transition linewidths of the source and sample. The SEDM fit indicates that only part of the hyperfine field distribution is being probed by the SEDM experiment as the apparent width of the SEDM line is 0.24 ± 0.01 mm/s, (obtained by simply fitting the SEDM spectrum with a single Lorentzian line) much narrower than the 0.71 ± 0.02 mm/s obtained using the same procedure on a transmission spectrum. This is direct evidence that static disorder can be detected using SEDM spectroscopy, and that a small sub-set of that disorder can be probed.

The presence of magnetic relaxation complicates the lineshape further. To describe SEDM spectra of a system with magnetic relaxation, we limit ourselves to an approach which is valid only for excitation on resonance. The more general case of a scattering lineshape with time dependent fields has not yet been solved.

To facilitate comparison of relaxation rates obtained with the models for magnetic relaxation which we have applied to transmission spectra [7,4,5], we start with the line shape function [16]:

$$I(E, E_i) = 2\Re(\mathbf{W}\underline{M}^{-1}\vec{1}). \tag{4}$$

with

$$W = \begin{pmatrix} P_1 \\ P_2 \end{pmatrix}$$

$$M = \begin{pmatrix} -\imath(E + E_i) + R + \Gamma/2 & -R \\ -R & -\imath(E - E_i) + R + \Gamma/2 \end{pmatrix} \tag{5}$$

where $R = \nu$ is the relaxation rate between states, E is the energy of the scattered radiation, E_i is the pump energy, and Γ is the linewidth of the sample. $I(E)$ describes the scattered radiation from the sample. Unlike the transmission situation, in a SEDM experiment, the initial and final populations of the two excited states during the time-dependent process must be averaged over the lifetime of the Mössbauer nucleus. Since we are using a Markovian argument to describe the relaxation process, if one state is initially populated and we consider either state to be equally likely at equilibrium, we have an initial estimate of the populations for the two levels (i.e. corresponding to 0° and 180° moment orientations) given by [17]

$$
\begin{aligned}
P_1 &= \frac{1}{2}(1+\exp(-2Rt)) \\
P_2 &= \frac{1}{2}(1-\exp(-2Rt))
\end{aligned}
\tag{6}
$$

We see that, with time, as P_1 decreases, P_2 increases, until each are $\frac{1}{2}$. Averaging over the nuclear lifetime [13,17], we have

$$
\begin{aligned}
P_1 &= \frac{R+\Gamma/2}{2R+\Gamma/2} \\
P_2 &= \frac{R}{2R+\Gamma/2}
\end{aligned}
\tag{7}
$$

which defines our W in Eqn. 5. Radiation emitted by nuclei returning to the ground state from each of these two excited states leads to two lines in the SEDM spectrum. The drive-line at the pump energy, and an echo-line in the line #6 position.

The result of the lineshape for relaxation between two sublevels is:

$$
\begin{aligned}
&I(E,S) = \frac{(\Gamma_D/2)^2}{E^2-(\Gamma_D/2)^2}\times \\
&\left(\sum_{i=1}^{6} I(E,E_i)\times\frac{W_{i,i}(\alpha)(\Gamma_b/2)^2}{(E-S)^2+(\Gamma_b/2)^2}+\right. \\
&\sum_{i=2}^{3} I(E,E_i)\times\frac{W_{i,i+2}(\alpha)(\Gamma_b/2)^2}{(E-S-G)^2+(\Gamma_b/2)^2}+ \\
&\left.\sum_{i=2}^{3} I(E,E_i)\times\frac{W_{i+2,i}(\alpha)(\Gamma_b/2)^2}{(E-S+G)^2+(\Gamma_b/2)^2}\right)
\end{aligned}
\tag{8}
$$

In Fig. 5 we show the calculated SEDM lineshapes for different values of the relaxation rate, ν. In general, the relative areas of the two peaks depends on the ratio of the relaxation rate to the nuclear lifetime (ν/Γ) and the observed lines will be broadened according to the ratio of the relaxation rate to the energy splitting (ν/E_i), just as in conventional transmission spectra. An additional symmetry breaking signature of magnetic relaxation is evident in the calculated SEDM spectra: With increasing ν the apparent linewidth of the echo-line becomes broader than the drive-line (see Fig. 5).

The predicted lineshape shown in Fig. 5 is in excellent agreement with the measured SEDM spectrum of a magnetic system experiencing spin flips (bottom panel in Fig. 2). With E_1 measured from the 80 K transmission Mössbauer spectrum of the ferrofluid, fitted parameters are Γ, the spin flip relaxation rate (ν), and baseline and an intensity scale factor. A complete description of the SEDM spectrum in the presence of relaxation accounts for both the relative line intensities and observed widths using only the relaxation rate ν. With the dynamics properly accounted for, the fitted value of Γ should equal Γ_s, the instrumental width determined from static samples.

IV. BELOW THE BLOCKING TEMPERATURE - COLLECTIVE EXCITATIONS

At the lowest temperatures, the magnetic moments of single-domain particles are fixed along their easy axes. No time-dependent magnetism is present and any magnetic disorder is static in nature, arising from the distribution of particle sizes and defects introduced by the chemical or grinding process used in preparation of the fine particle system.

When the left-most line (line #1, $m_g = -\frac{1}{2} \rightarrow m_e = -\frac{3}{2}$ transition) is driven, the $m_e = -\frac{3}{2}$ sublevel is selectively populated. In a static magnetic environment, the radiation is re-emitted when the excited Mössbauer nucleus decays, to the $m_g = -\frac{1}{2}$ ground state. This has been confirmed with α-Fe [9], a-$Fe_{80}B_{20}$ [7,9], and $Fe_{65}Ni_{35}$ [7]. The low temperature transmission Mössbauer spectra of the ferrofluids (e.g. 12 K and 20 K in Fig. 6) could be fitted with the multi-level model and were consistent with static disorder. The 20 K SEDM spectra of the ferrofluids (Figs. 7 and 8) are in agreement with this analysis of the low temperature transmission Mössbauer spectra. A single line in the SEDM spectra, at the pump energy, with an apparent linewidth that is greater than that for α-Fe (upper panels of

Fig. 9 and 10) is the demonstrated signature of static disorder (apparent linewidths of the ferrofluid spectra are comparable to that observed for a-$Fe_{80}B_{20}$). The additional linewidth is fully accounted for using the hyperfine field distribution, $P(B_{hf})$ derived from transmission Mössbauer spectra. Using Eqn. 3, with $P(B_{hf})$ for the 20 K and 25 K spectra of both the 4.5 nm and 6.0 nm ferrofluids, fitted linewidths indicated by the $\bigtriangledown$ in Figs. 9 (4.0 nm ferrofluid) and 10 (6.5 nm ferrofluid) are consistent with the instrumental linewidth, Γ_s. These results clearly indicate that only static disorder is present at 20 and 25 K.

With an increase in temperature, moments of single-domain particles may begin to fluctuate around their easy axes. This time-dependent magnetic behavior, called collective excitations [2], is assumed to happen faster then the Larmor precession of Mössbauer atoms. This has been confirmed with ZF-μSR experiments on a magnetic fine particle system [10], described below, where collective excitations are observed to have a fluctuation frequency of $\sim$ 40 MHz. This is faster than the $\sim$ 10 MHz Larmor precession frequency of Mössbauer atoms, however, not fast enough for Mössbauer spectra to show motional narrowing effects (i.e. a six-line transmission Mössbauer spectra is clearly observed). The combined effects of disorder due to the distribution of particle sizes and collective excitations results in a subtle but clear effect on Mössbauer spectra.

Collective magnetic excitations, which according to the multi-level transmission Mössbauer spectra model, occur at temperatures below T_B, lead to an increase in the apparent width of line #1 in the SEDM spectra of the ferrofluids (Figs. 7 and 8). This increase is beyond that which can be accounted for using the observed static disorder in the transmission spectra. This broadening happens above 25 K for the 4.5 nm ferrofluid and above 30 K in the 6.0 nm ferrofluid (Figs. 9 and 10). If the line broadening of the spectrum at each temperature (where only line #1 is present) is assumed to be due simply to static disorder (i.e. using Eqn. 3), fitted linewidths of $\Gamma = 0.20 \pm 0.01$ mm/s for the 4.5 nm ferrofluid ($\bigtriangledown$ in Fig. 9 at 30 K), and $\Gamma = 0.215 \pm 0.005$ mm/s for the 6.0 nm ferrofluid ($\bigtriangledown$ in Fig. 10 at 50 K), are obtained. These are in striking conflict with the $\Gamma_s = 0.165 \pm 0.002$ mm/s of the a-$Fe_{80}B_{20}$ alloy and $\Gamma_s = 0.167 \pm 0.005$ mm/s for the $Fe_{65}Ni_{35}$ alloy [7] that were completely characterized by a distribution of static hyperfine fields. The fitted Γ's of the ferrofluids, obtained assuming only static disorder, are too large to simply reflect the effects of the lifetime of the Mössbauer nucleus excited state and instrumental broadening. This clear increase in apparent linewidth caused by collective excitations serves to underline the exquisite sensitivity of SEDM to dynamic effects.

Additional information on collective excitations in magnetic fine particle systems comes from ZF-μSR spectra of a polysaccharide iron complex (PIC) [10]. As PIC is a synthetic complex of akaganéite with a carbohydrate shell it is plausible to expect one contribution to the μSR lineshape from the carbohydrate shell and an other contribution from the akaganéite core. The ZF-μSR was therefore fitted as the sum of two components [10]. Approximately half of the muons stop in the shell and give a slow, exponential decay ($\lambda_2 \sim 0.6$ MHz in Fig. 11), while the remainder come to rest in the core where they experience a significant static field and their signal could be fitted using a conventional Kubo-Toyabe form [6]:

$$G_z(\Delta) = \frac{1}{3} + \frac{2}{3}(1 - (\Delta t)^2)\exp\left(-\frac{(\Delta t)^2}{2}\right)$$

where Δ/γ_μ is the average field at the muon site and γ_μ is the gyromagnetic ration of the muon. If the muons in the core are also affected by magnetic fluctuations, then the one-third tail of the Kubo-Toyabe function will also exhibit an exponential decay ($\lambda_1 \sim 40$ MHz in Fig. 11).

As the blocking temperature of the PIC is $T_B = 10 \pm 2.5$ K [10], spin dynamics in the iron core of the PIC at temperatures below 10 K consist of particle moments undergoing collective excitations. These collective excitations result in $\lambda_1 \sim$40 MHz. As the muon is sensitive to a wider range of measuring frequencies, collective excitations, which are largely washed out by the $\sim$10 MHz measuring frequency of the Mössbauer effect, exhibit dynamic behavior with μSR. This is consistent with Mørup's collective excitation model which assumes that the moment fluctuations are faster than the Mössbauer effect measuring frequency [2].

Although λ_1 due to collective excitations in the cores was found to be largely temperature independent below $T_B \sim 10$ K, not all of the one-third tail was lost at low temperatures.

This behavior led to a zero-offset in the μSR data. The static contribution from the cores was therefore further resolved into two components with the same value for Δ: one exhibiting an exponential decay characterized by λ_1, and the second completely static with no further decay. The fraction of muons that came to rest in purely static environments is shown as a function of temperature in the lower panel of Fig. 11. The static core fraction starts out near 100% at 2 K, i.e. even the collective excitations are mostly frozen out. With increasing temperature more of the cores start experiencing collective excitations and the static fraction falls. It is interesting to note that even as the fraction of cores exhibiting collective excitations is increasing, the average fluctuation rate (λ_1) is essentially unchanged. Furthermore, at 20 K or *twice* the blocking temperature, 30% of the cores are still completely static. This behavior results from the broad particle size distribution present in the PIC sample but also serves to underline the need for a complete description of a magnetic fine particle system where fully static moments, collective excitations and particles undergoing superparamagnetic spin flips may all be present in significant concentrations.

V. ABOVE THE BLOCKING TEMPERATURE - SUPERPARAMAGNETISM

With a further increase in temperature, above the blocking temperature of single domain particles, moments begin to undergo 180° flips. Superparamagnetic spin-flips in a magnetic fine particle system have the most dramatic effect on the SEDM spectra: For the 4.5 nm ferrofluid (Fig. 7) a new line is clearly present at 30 K, and for the 6.0 nm ferrofluid (Fig. 8) at 70 K a new line is distinct in the SEDM spectrum. These lines at $\sim +8$ mm/s, are due to the $m_e = +\frac{3}{2} \rightarrow m_g = +\frac{1}{2}$ (line #6) transition, and are present even though we have explicitly populated only the $m_e = -\frac{3}{2}$ excited state. This is possible because when a spin flip occurs in a particle in which we have pumped a nucleus into the $m_e = -\frac{3}{2}$ excited state, the field within that particle reverses, the projection of I_e onto that field changes sign, and the populated state becomes $m_e = +\frac{3}{2}$. This state then decays to give the line at $\sim +8$ mm/s. The observation of a relatively sharp line at $\sim +8$ mm/s indicates that the moment reversal is effectively instantaneous on the time-scale of the SEDM measurement. The intensity ratio of the lines at ~ -8 mm/s and $\sim +8$ mm/s is related to the probability that a spin flip occurs during the lifetime of the excited state and thus is a direct indication of the rate at which spin flips are occurring. We must emphasize that no amount of *static* disorder can lead to the appearance of line #6 in the spectra. It can *only* be caused by magnetization reversals.

Superparamagnetic spin flips occur with increasing frequency above T_B. Blocking temperatures of $T_B = 25 \pm 2$ K for the 4.5 nm ferrofluid and $T_B = 54 \pm 3$ K for the 6.0 nm ferrofluid are determined from linear fits to the temperature dependence of the SEDM relaxation rates determined from the SEDM spectra at each temperature fitted with Eqn. 8. These T_B's are in excellent agreement with transmission Mössbauer ($T_B = 30 \pm 5$ for the 4.5 nm ferrofluid, $T_B = 50 \pm 5$ for the 6.0 nm ferrofluid) and frequency dependent χ_{ac} measurements of T_B [5].

It is clear that the linewidths returned by the single-frequency relaxation function (Eqn. 8) are significantly broader than Γ_s (see □ in Figs. 9 and 10). This is because the effects of the static disorder are not explicitly included in the model and are simply accounted for by allowing the fitted linewidth to increase. It is interesting to note that in both ferrofluid samples, the onset of collective excitations is clearly visible as in increase in fitted linewidth. Near T_B, where the superparamagnetic spin flips are relatively infrequent, the single-frequency model (Eqn. 8) correctly describes the SEDM spectra, however, as we move further above T_B, and the flip frequency exceeds $\sim$4 MHz, the fitted linewidth starts to increase. The continued increase in the fitted linewidth describing the two SEDM lines as the relaxation rate increases indicates that our model is too simple. A correct description of the superparamagnetic processes should involve no *fitted* linewidth variations.

A range of relaxation rates (one for each particle size) was used in the multi-level relaxation model developed to fit the transmission Mössbauer spectra [5] of ferrofluids. Since the transmission experiments are sensitive to moment flips that are about or above the Larmor frequency and SEDM is sensitive to moment flips that are about or below the Larmor frequency, relaxation rates from the transmission Mössbauer spectra multi-level model within the time scale of the SEDM measurement can be used to fit the SEDM spectra. With this range of relaxation rates derived from the transmission Mössbauer multi-level fits and Eqn. 8, a SEDM ferrofluid model was used to fit the spectra above T_B that could not be fitted assuming a single relaxation rate. These fits are shown ($\triangle$) in Figs. 9 and 10 and a more consistent linewidth results. At these higher temperatures, well above T_B, the SEDM spectra are sensitive to a range of different sized particle moments undergoing spin-flips.

VI. CONCLUSIONS

Superparamagnetic spin flips have been explicitly detected and model independent relaxation rates have been determined using SEDM spectroscopy on 4.5 nm and 6.0 nm ferrofluids. The fits to the SEDM ferrofluid spectra provide *model-independent* measurements of relaxation rates of single domain particles, and the model-independent measurement of collective excitation has been made. Agreement between SEDM relaxation rates and transmission Mössbauer spectra multi-level fits further support our model [5]. This observation of collective excitations is consistent with ZF-μSR results on PIC.

This work was supported by grants from the Natural Sciences and Engineering Research Council of Canada and Fonds pour la formation de chercheurs et l'aide à la recherche, Québec.

REFERENCES

[1] current address: Materials and Chemical Sciences Division, Energy Sciences and Technology Department, Brookhaven National Laboratory, Upton, N.Y., 11973-5000.

[2] S. Mørup, J. Magn. Magn. Mater. **37**, 39 (1983).

[3] J.L. Dormann, D. Fiorani and E. Tronc, in "*Advances in Chemical Physics*", **XCVIII**, eds. I. Prigogine and Stuart A. Rice (John Wiley & Sons, Inc., New York), 283 (1997).

[4] J. van Lierop and D.H. Ryan, J. Appl. Phys. **87**, 6277 (2000).

[5] J. van Lierop and D.H. Ryan, Phys. Rev. B. **63**, 064406 (2001).

[6] R. Kubo and T. Toyabe, in *Magnetic Resonance and Relaxation* edited by R. Blinc, (North-Holland, Amsterdam, 1967), p. 810.

[7] J. van Lierop and D.H. Ryan, J. Appl. Phys. **85**, 4518 (1999).

[8] J. van Lierop and D.H. Ryan, Phys. Rev. Lett. **85**, 3021 (2000).

[9] J. van Lierop and D.H. Ryan, Rev. Sci. Instrum. **72**, 3349 (2001).

[10] J. van Lierop, D.H. Ryan, M. Pumarol and M. Roseman, J. Appl. Phys. **89**, 7645 (2001).

[11] Ferrofluidics Corporation, 40 Simon Street Nashua, N.H., U.S.A., 03061.

[12] W.T. Coffey, D.S.F. Crothers, Yu. P. Kalmykov, E.S. Massawe and J.T. Waldron, Phys. Rev. E, **49**, 1869 (1994).

[13] Bohdan Balko and Gilbert R. Hoy, Phys. Rev. B **10**, 36 (1974).

[14] Neil D. Heiman and J.C. Walker, Phys. Rev. **184**, 281 (1969).

[15] P. Gütlich, L. Rainer and A. Trautwein in *Mössbauer Spectroscopy and Transition Metal Chemistry*, Springer-Verlag, Berlin, 1978.

[16] R.A. Sack, Molec. Phys. **1**, 163 (1958).

[17] A. Paupolis in *Probability, Random Variables, and Stochastic Processes*, McGraw-Hill, New York, 1965.

FIGURES

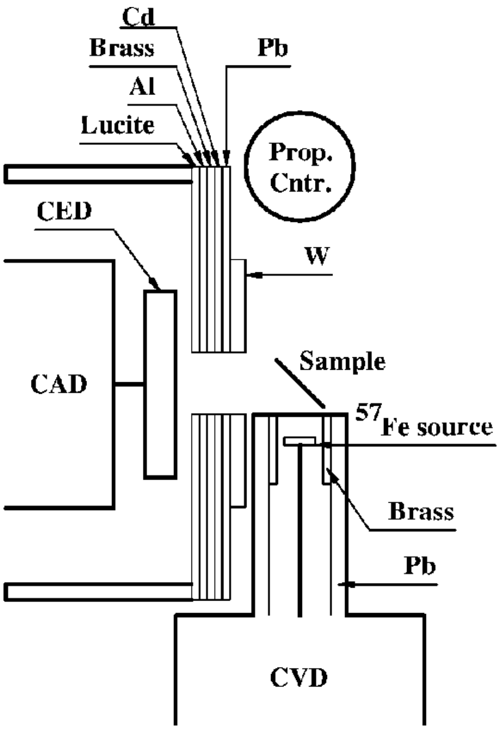

FIG. 1. Schematic block diagram of the SEDM apparatus.

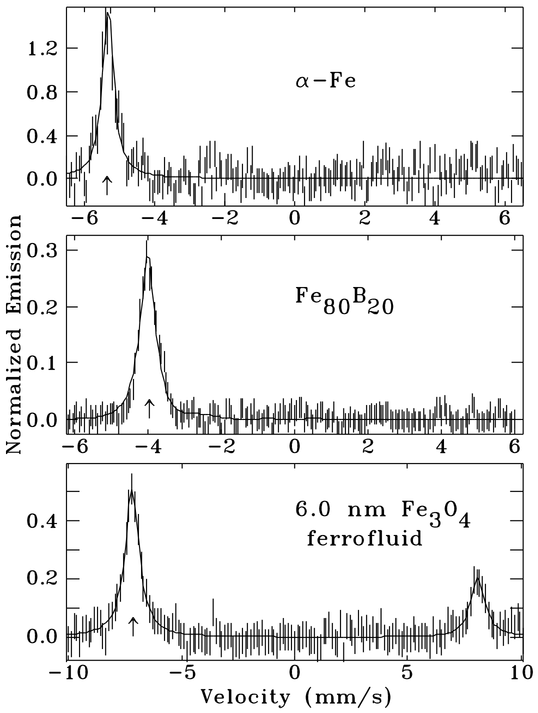

FIG. 2. SEDM spectra when line #1 is pumped in α-Fe at room temperature (top), a-$Fe_{80}B_{20}$ at room temperature (middle), and the 6.0 nm ferrofluid at 80 K (bottom). Solid lines are fits to lineshapes described in the text. Driven lines indicated by the $\uparrow$.

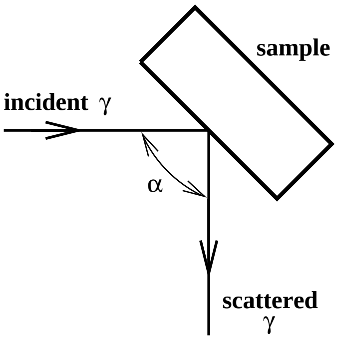

FIG. 3. Sample orientation relative to the incident and scattered radiation directions in a SEDM experiment.

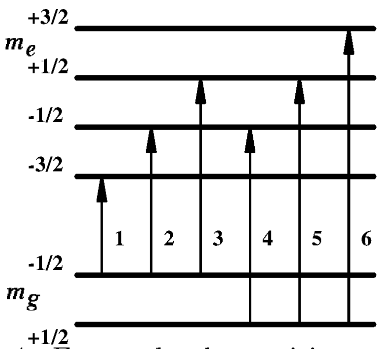

FIG. 4. Energy level transitions and the corresponding spectra line number associated with them.

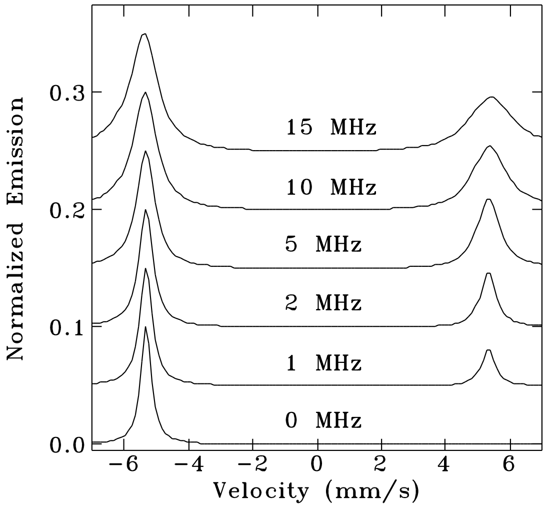

FIG. 5. Lineshapes for different values of relaxation rate ν and fixed Γ.

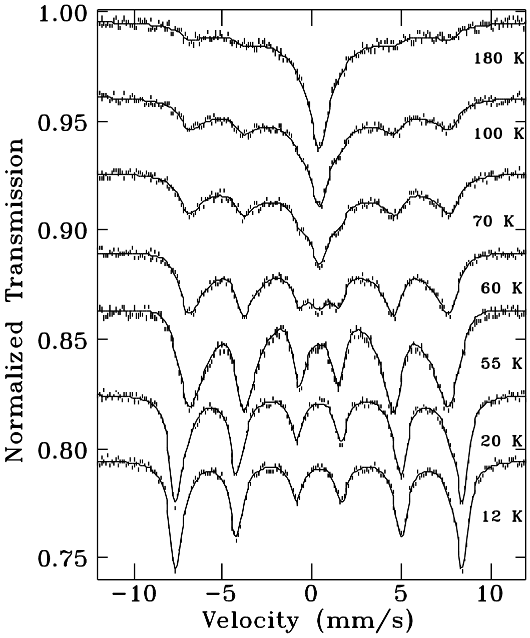

FIG. 6. Transmission spectra of the 6.0 nm ferrofluid.

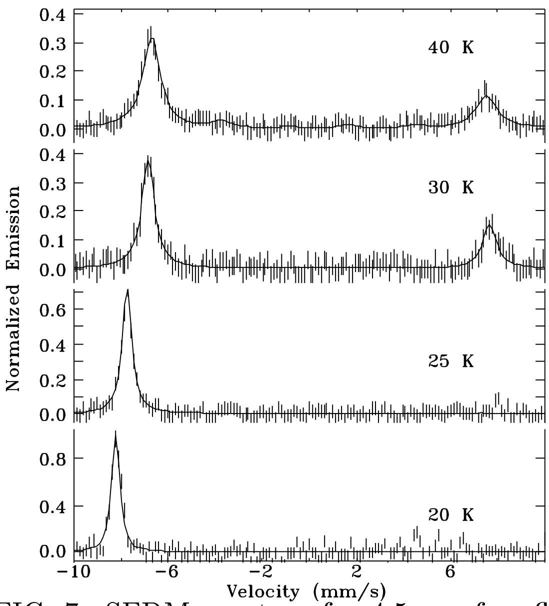

FIG. 7. SEDM spectra of a 4.5 nm ferrofluid. At each temperature, the pump energy was centered on the line at the left. The appearance of the peak at positive velocities indicates the onset of superparamagnetic moment reversals.

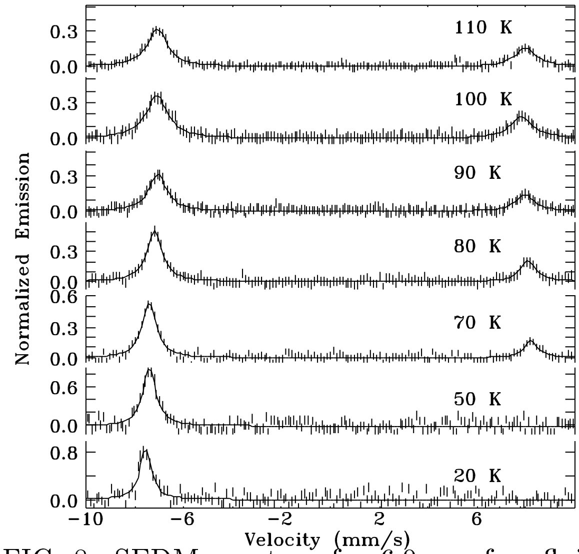

FIG. 8. SEDM spectra of a 6.0 nm ferrofluid. At each temperature, the pump energy was centered on the line at the left. The appearance of the peak at positive velocities indicates the onset of superparamagnetic moment reversals.

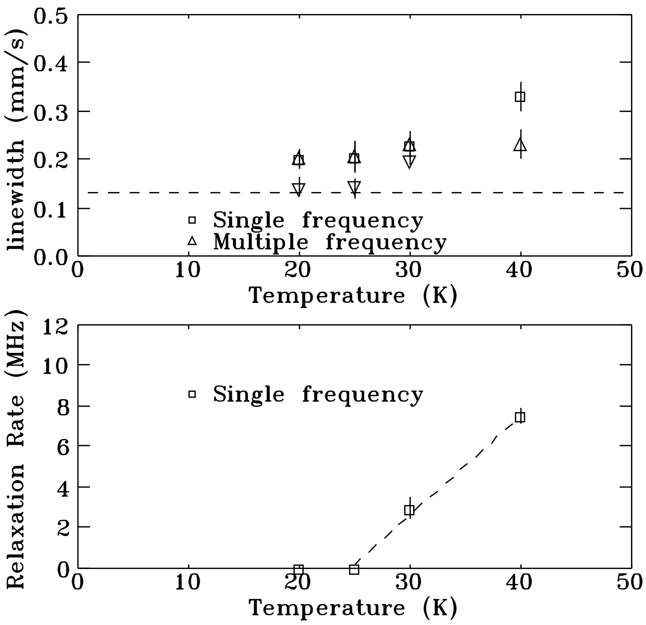

FIG. 9. Relaxation rates (lower panel) show the onset of superparamagnetic spin-flips above T_B=25±2 K for the 4.5 nm ferrofluid. The upper panel shows fitted linewidths derived from three different models. At the lowest temperatures, a model (Eqn. 3) incorporating only static disorder ($\bigtriangledown$) shows the onset of collective excitations at 30 K. A single-frequency model ($\square$, Eqn. 8) shows the onset of superparamagnetic spin flips above T_B, but also yields an increasing fitted linewidth. The more complete model ($\triangle$) that includes a distribution of relaxation rates, gives a proper description of the spectra without an increasing fitted linewidth (see text). The dashed line shows the instrumental linewidth Γ_s.

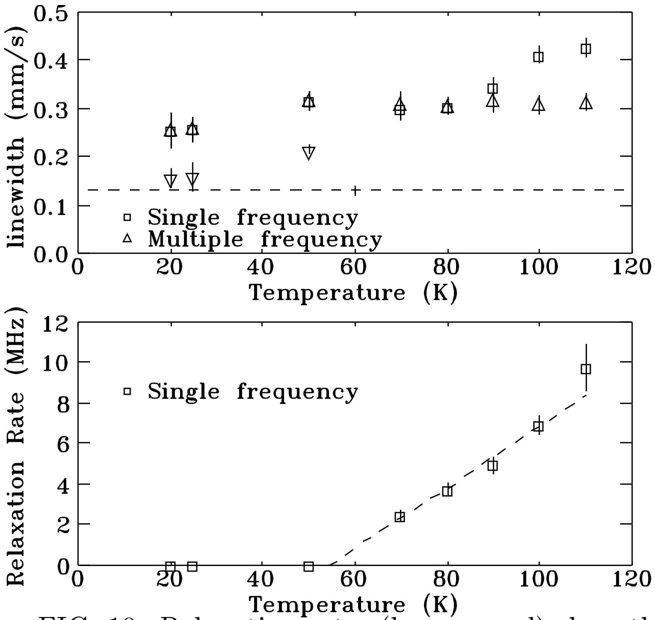

FIG. 10. Relaxation rates (lower panel) show the onset of superparamagnetic spin-flips above T_B=54±3 K for the 6.0 nm ferrofluid. The upper panel shows fitted linewidths derived from three different models (see caption of Fig. 9 for details). The dashed line shows the instrumental linewidth Γ_s.

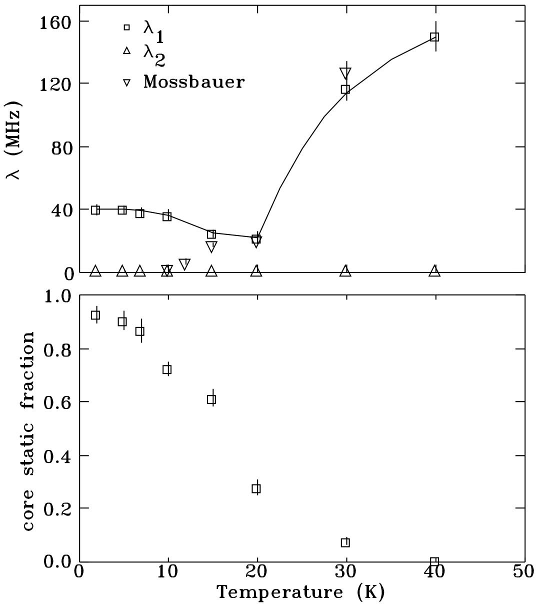

FIG. 11. Top: Temperature dependence of the fitted ZF-μSR dynamic (λ) relaxation rates in PIC. The increase in λ_1 indicate when moments begin to unblock at T_B. Notice the agreement of relaxation rates from the μSR ($\square$) and transmission Mössbauer fits ($\triangle$). λ_2 denotes the slow muon fluctuations in the PIC's carbohydrate shell. The solid line is a guide to the eye. Bottom: Fraction of static, blocked moments in the PIC fitted from the zero-offset of the ZF-μSR spectra.